

Tungsten Catalysts Supported on Activated Carbon

I. Preparation and Characterization after Their Heat Treatments in Inert Atmosphere

M. A. Alvarez-Merino,* F. Carrasco-Marín,* J. L. G. Fierro,† and C. Moreno-Castilla*¹

*Departamento de Química Inorgánica, Facultad de Ciencias, Universidad de Granada, 18071 Granada, Spain; and †Instituto de Catálisis y Petroleoquímica, CSIC, Cantoblanco, 28049 Madrid, Spain

Received October 25, 1999; revised February 1, 2000; accepted February 10, 2000

Tungsten catalysts supported on activated carbon, and with different metal content, were prepared from both ammonium tungstate and tungsten hexacarbonyl precursors. The catalysts were subjected to heat treatments, in He flow, between 623 and 1223 K for 4 h and characterized to determine their surface area and pore texture, the chemical state and dispersion of the metallic phase, and the total surface acidity. For this purpose, different techniques were used such as adsorption of N₂ at 77 K and mercury porosimetry; X-ray diffraction and X-ray photoelectron spectroscopy; temperature-programmed desorption of previously adsorbed NH₃; and behavior in the decomposition reactions of isopropanol. Results show that in the case of the catalysts prepared from ammonium tungstate an increase in the treatment temperature between 623 and 1223 K leads to a drop in the O/W ratio to below 3, resulting in the appearance of nonstoichiometric oxides such as W₂₅O₇₃, W₂₀O₅₈, and W₁₈O₄₉. At 1223 K, a mixture of W, tungsten carbides, and tungsten trioxide was detected. The catalysts prepared from tungsten hexacarbonyl presented a higher dispersion and no X-ray diffraction peaks. Total surface acidity, as measured by ammonia desorption, decreased with increasing treatment temperature, and the study of the decomposition reactions of isopropanol showed that the catalysts were essentially of acid character, with a much higher selectivity (or rate) to propene than to acetone. Moreover, there was a linear relationship between the reaction rate to propene and the amount of NH₃ desorbed from the catalysts, irrespective the method of preparation and treatment temperature. © 2000 Academic Press

Key Words: tungsten catalysts; carbon support; total surface acidity.

INTRODUCTION

Supported catalysts based on tungsten oxide show many applications in heterogeneous catalysis. Thus, they are widely used in several reactions of industrial importance such as hydrotreatments, hydrocracking of heavy fractions from oil, dehydration of alcohols, metathesis, and isomer-

ization of olefins (1–12). The supports used with this oxide are mainly Al₂O₃ and TiO₂ (8, 10, 13–28), although other supports such as SiO₂ (29–31), MgO (32), and MgF₂ (6) were also used. In these cases, aqueous solutions of either tungstate, metatungstate, or paratungstate were used to prepare the supported catalysts. After preparation, the catalysts were generally calcined in dried air at temperatures between 723 and 773 K. The knowledge of the structure and the factors controlling the active phase is important for the subsequent development and optimization of the catalytic system formed by the supported metal oxide. However, characterization of the molecular structure of these catalysts can be complicated since the metal oxide can have different molecular structures and oxidation states, which depend on the type of support, metal oxide loading, gaseous environment, and treatment temperature (24).

Hercules *et al.* (15) studied tungsten oxide/Al₂O₃ catalysts by different techniques and concluded that the molecular structure of the active phase depended on the amount of tungsten oxide deposited. Thus, for low percentages tetrahedral (WO₄) units were detected, for 15–24% of WO₃ octahedral (WO₆) polymeric units were observed, and above the monolayer, which is obtained for 24% of WO₃, bulk WO₃ crystals were developed. Wachs *et al.* (18) also noticed that in tungsten oxide/Al₂O₃ catalysts the symmetry of the environment depended on the surface coverage and the presence of coordinated water. Hilbrig *et al.* (22) also studied the tungsten oxide catalysts supported on γ -Al₂O₃-C and TiO₂ (75% anastase and 25% rutile). The tungsten oxide on both supports was present as tetrahedral (WO₄) and pentahedral (WO₅) units in the dehydrated state after treatment at 673 K. After water adsorption, all surface W atoms were octahedrally coordinated. This structure was independent of the support, the tungsten oxide content, and the preparation method of the catalyst. The tungsten oxide/TiO₂ system was also studied by Wachs *et al.* (21) who observed tetrahedral WO₄ units for low tungsten oxide contents, whereas at high metal oxide contents

¹ To whom correspondence should be addressed. Fax: 34-958-248526. E-mail: cmoreno@ugr.es.



octahedral WO_6 units, forming polytungstates, together with crystalline WO_3 appeared. Using Raman spectroscopy and XPS, Hercules *et al.* (25) showed up to three different tungsten species in the tungsten oxide/ TiO_2 catalysts, depending on the metal oxide content. Finally, Wachs (31) indicated that, under normal conditions and when the surface was hydrated, the molecular structures of the metal oxide surface species were determined by the pH of the point of zero charge (pH_{PZC}) of the metal oxide–support system. Thus, it has been observed (10) that on Al_2O_3 and TiO_2 , with pH_{PZC} of 8.5–9 and 6, respectively, tetrahedral units are preferentially developed on alumina and octahedral units mainly on titania. All these results show that the surface molecular structure of the supported tungsten oxide is quite complex and depends on the metal oxide content, the presence of humidity, and the pH_{PZC} of the support.

On the other hand, there are very few studies of tungsten oxide catalysts supported on carbon materials despite their importance as supports for catalysts (33). One recent study (34) focuses on the preparation and use of group 6 metal oxide–carbon aerogels in the skeletal isomerization of 1-butene and in another work the activity of sulfided W/C catalysts in reactions such as the dehydrodesulfuration of thiophene and hydrogenation of butene (35) is studied. Accordingly, we decided to study tungsten oxide catalysts supported on an activated carbon. For this purpose, tungsten oxide catalysts with different metal content were prepared by using either ammonium tungstate or tungsten hexacarbonyl precursors, which were deposited on an activated carbon prepared in the laboratory from almond shells. The catalysts so prepared were treated at different temperatures in He flow and characterized by different techniques in order to evaluate textural properties, chemical composition, dispersion, and surface acidity.

EXPERIMENTAL

The activated carbon used was prepared from almond shells. Previously they were ground and sieved to obtain a particle size from 1.40 to 2.38 mm. Subsequently, they were carbonized in N_2 flow at 1123 K for 1 h and steam activated at 1023 K for 13 h as explained in detail elsewhere (36). The burn-off of the carbonized sample during its activation was around 40%. The activated carbon so obtained was sieved again and the particle size between 1–2 mm was used. This sample, with an ash content of 0.1%, will be referred to in the text as S.

The catalysts were prepared either from ammonium tungstate or tungsten hexacarbonyl precursors. In the first case, the support was impregnated with an aqueous solution of the tungsten compound to obtain four catalysts containing 4.8, 9.1, 14.9, and 23.1% W. The catalysts with the higher metal content were prepared by successive impregnations,

drying between them the impregnates at 383 K. When $\text{W}(\text{CO})_6$ was used as a catalyst precursor, a sublimation technique was followed, as described elsewhere (37, 38). For this purpose, the powdered carbonyl was mixed with the appropriate amount of support in a glass tubing, which was sealed under vacuum (10^{-3} Torr; 1 Torr = 133.3 N m^{-2}). This closed reactor was mechanically rotated for about 4 h at a temperature close to 343 K to force the carbonyl to sublime evenly onto the support. After cooling to room temperature, the supported catalysts were sieved in order to remove the finest particles produced during the preparation procedure. Two catalysts containing 6.1 and 15.1% W were prepared by following this procedure.

The exact tungsten content of the supported catalysts was determined in a thermobalance by burning, in a flow of air, a portion of the catalysts at 1073 K until constant weight. The catalysts prepared from ammonium tungstate will be referred to in the text as W, and those prepared from the carbonyl as HW. In both cases the tungsten content of the catalysts will follow the letters W or HW.

Before characterization, the catalysts were heated in a He flow, at 2 K min^{-1} , to temperatures ranging from 623 to 1223 K and then holding the maximum temperature for 4 h. Both the support and some selected catalysts were characterized, to determine their surface area and pore texture, by N_2 adsorption at 77 K and mercury porosimetry up to 4190 kg cm^{-2} . In this case a mercury porosimeter, Quantachrome model Autoscan 60, was used, which allowed the volume of pores wider than 3.6 nm to be measured. The pH_{PZC} of the support was measured by the so-called pH drift method which was described in detail elsewhere (39). A pH_{PZC} of 10.2 was recorded.

Temperature-programmed desorption (TPD) was carried out by heating the samples at different temperatures up to a maximum of 1273 K in a He flow at heating rates of either 10 or 20 K min^{-1} and recording the amount of gases evolved with a quadrupole mass spectrometer (Balzers, model Thermocube) as a function of temperature as described elsewhere (40). X-ray diffraction (XRD) patterns were recorded with a Phillips PW1710 diffractometer using $\text{Cu K}\alpha$ radiation. The JCPDS files were used to assign the different diffraction peaks observed.

X-ray photoelectron spectroscopy measurements (XPS) were carried out with a VG Escalab 200 R with $\text{Mg K}\alpha$ source ($h\nu = 1253.6 \text{ eV}$) and hemispherical electron analyzer. Prior to analysis, the samples were heated *in situ* at temperatures equal to or below 748 K in He flow. When the temperature of the heat treatment was higher than 748 K, the treatment was carried out in a quartz reactor under He flow. Once the treatment was finished, the sample was cooled to room temperature under the He flow, impregnated with *n*-octane, and then transferred to the pretreatment chamber of the XPS instrument. After the *in situ* heat treatment all the samples were evacuated at high vacuum and room temperature, and then introduced in the analysis

chamber. A base pressure of 10^{-9} Torr was maintained during data acquisition. Survey and multiregion spectra were recorded at C_{1s} , O_{1s} , and W_{4f} photoelectron peaks. Each spectral region of photoelectron interest was scanned several times to obtain good signal-to-noise ratios. The spectra obtained, once the background signal was corrected, were fitted to Lorentzian and Gaussian curves to obtain the number of components, the position of the peaks, and the peak areas.

The total surface acidity of the supported catalysts was determined by TPD of previously adsorbed NH_3 (41–47). The catalysts were heated in He flow ($60 \text{ cm}^3 \text{ min}^{-1}$) to the maximum temperature, ranging between 623 and 1223 K, and held for 4 h. After that, the sample was cooled to 373 K in flowing He, and then the He flow was switched to NH_3 flow at a rate of $30 \text{ cm}^3 \text{ min}^{-1}$ over 30 min. After this time, the NH_3 flow was again switched to He, which was flowed through the catalyst for 30 min, in order to purge the lines and reactor and to remove the ammonia physisorbed on the catalyst. TPD of the strongly adsorbed ammonia was carried out by heating the catalyst from 373 to 973 K in He flow, at a heating rate of 10 K min^{-1} , and recording the amount of NH_3 evolved as a function of temperature.

Surface acidity of the supported catalysts was also evaluated by studying the decomposition reactions of isopropanol (48–51). Catalytic tests were carried out in a glass microreactor working at atmospheric pressure with 0.2 g of catalyst. The reaction was performed in a He flow saturated with isopropanol at 273 K. The total flow rate was $62 \text{ cm}^3 \text{ min}^{-1}$ and the partial pressure of the alcohol 8.44 Torr. The reaction temperature was 383 K and the analysis of the reaction products was done by online gas chromatography using a Perkin Elmer gas chromatograph, model 8500, with flame ionization detector and a column Carbopack B80/120. Prior to reaction the catalysts were heated, in He flow, at temperatures between 623 and 1223 K for 4 h.

RESULTS AND DISCUSSION

The catalysts from the W series were prepared by impregnation of the support with an aqueous solution of ammonium tungstate at a pH of 6.3, which would favor the formation of paratungstate (52). Due to the high surface basicity of the support, with a pH_{PZC} of 10.2, this favors not only the adsorption of the different tungstate ions on the surface of the support, because at the solution pH it was positively charged, but also the formation of tetrahedral (WO_4) species (31).

The temperature-programmed decomposition of catalyst W23.1 was studied by heating the sample to 1273 K under He flow. The profiles obtained are depicted in Fig. 1. Figure 2 shows the same profiles obtained with the support (S) when treated under the same conditions. The H_2O profile of the catalyst showed three peaks at 375, 575, and

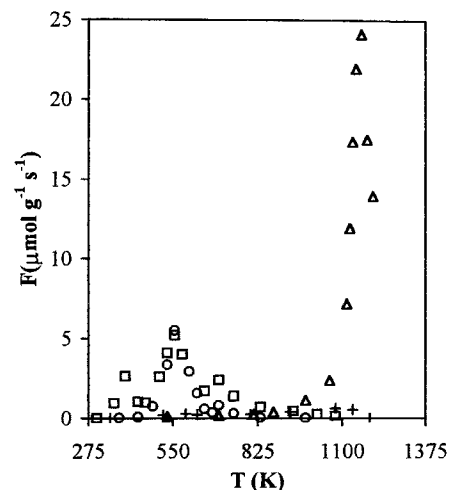


FIG. 1. TPD profiles of catalyst W23.1 heated at 50 K min^{-1} to 1273 K in He flow. \square , H_2O ; \circ , NH_3 ; \triangle , CO ; $+$, CO_2 .

725 K, with the peak at 575 K displaying the maximum intensity. The support also showed peaks at 375 and 575 K in the water adsorption profile. The NH_3 desorption profile of the catalyst showed an intense peak with maximum at 575 K and another weak peak at 725 K. From these results, it appears that the peak at 375 K corresponds to loss of the hydration water molecules coming from the ammonium tungstate, whereas the peaks at 575 and 725 K are associated with decomposition of the salt.

The CO evolution profile of the catalyst was different from that of the support. Thus, in the catalyst the maximum was placed at 1125 K and the intensity of the peak was around 6 times higher than in the case of the support. Production of a higher amount of CO in the supported catalyst than in the support was due to the reduction of tungsten

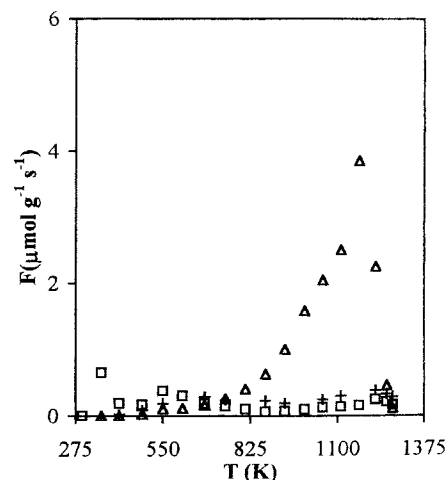


FIG. 2. TPD profiles of support heated at 50 K min^{-1} to 1273 K in He flow. \square , H_2O ; \triangle , CO ; $+$, CO_2 .

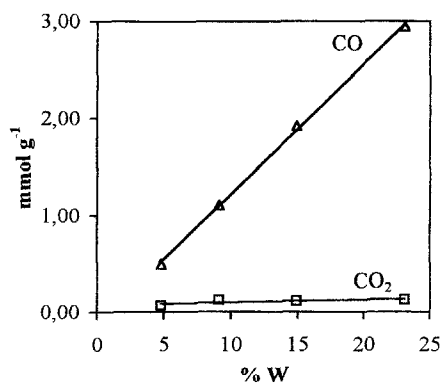


FIG. 3. Amounts of CO and CO₂ evolved up to 1273 K versus tungsten content in catalysts from series W.

oxide particles, formed after decomposition of ammonium tungstate by the carbon support. This reduction is thermodynamically favored (53) and will take place at the metal oxide-support interface. This reduction yields a metal oxide with an oxidation state below (VI) or even metallic tungsten. Figure 3 shows the amounts of CO and CO₂ evolved from the supported catalyst, once the respective amounts evolved from the support were subtracted, versus the tungsten content of the catalysts. The amount of CO evolved linearly increased with W content whereas the amount of CO₂ evolved is very low and practically independent of the W content. These results show again that the tungsten oxide particles were reduced by the support.

The temperature-programmed decomposition profiles of catalyst HW6.1 are depicted in Fig. 4. The amounts of H₂O and CO₂ evolved from the supported catalyst were similar to those evolved from the support, varying only in the amount of CO. The CO desorption profile had a symmetric peak at 475 K and another asymmetric one around 1125 K with a shoulder around 1175 K. Brenner *et al.* (54) found

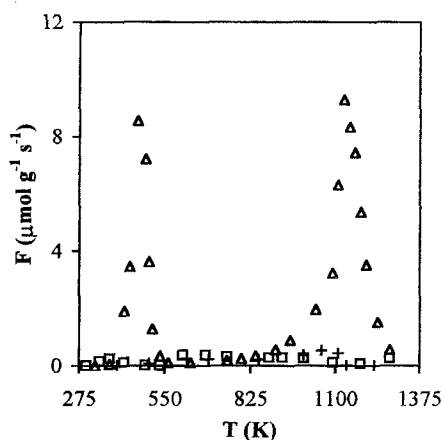


FIG. 4. TPD profiles of catalyst HW6.1 heated at 50 K min⁻¹ to 1273 K in He flow. □, H₂O; △, CO; +, CO₂.

that when W(CO)₆ was supported on TiO₂ dehydroxylated at 773 K, decarbonylation was completed by heating the catalyst between 473 and 523 K, yielding the metal in zero oxidation state. When Al₂O₃ was used as support, complete decarbonylation required a higher temperature, 673 K (55–57). If the amount of CO evolved from these catalysts is corrected with that evolved from the support, the amount of CO evolved from the catalysts was lower than that expected from the W content of the catalysts. Thus, up to 575 K, 26 and 57% was evolved from HW6.1 and HW15.1, respectively, and between 575 and 1273 K another 23 and 18% of the total of CO expected. These results indicate that either decarbonylation was not complete or the tungsten hexacarbonyl was partially decomposed during the preparation of the supported catalysts.

Surface Area and Porosity of the Support and Supported Catalysts

Surface area and porosity of the support and supported catalysts were studied by N₂ adsorption at 77 K and by mercury intrusion porosimetry. The BET equation was applied to N₂ adsorption isotherms, thus allowing the N₂ surface area (S_{N_2}) to be calculated. The volumes of pores with a diameter between 3.6 and 50 nm (V_2) and wider than 50 nm (V_3) were obtained by mercury porosimetry. The V_2 volume would be the mesopore volume, although, in fact, this volume would correspond to pores with a diameter between 2 and 50 nm (58). V_3 would correspond to the macropore volume. All these data are compiled in Tables 1 and 2 for the catalysts from series W and HW, respectively, heat treated at different temperatures in He flow. In these tables the surface characteristics of the support (S) are also included. The value of S_{N_2} of the support decreased when the amount of the tungsten precursor compound deposited in both series of catalysts, W and HW, increased. The mesopore volume slightly increased in the two series of catalysts for those with the lowest tungsten content heated at 748 K. However, for other tungsten contents and treatment temperatures both V_2 and V_3 decreased in comparison to the support.

TABLE 1

Surface Area and Porosity of Support and Supported Catalysts from Series W after Their Heat Treatments in He Flow at Different Temperatures for 4 h

Sample	Treatment	S_{N_2} , m ² g ⁻¹	V_2 , cm ³ g ⁻¹	V_3 , cm ³ g ⁻¹
S	—	929 ± 7	0.17	0.36
W4.8	He, 748 K	834 ± 6	0.20	0.33
W23.1	He, 748 K	576 ± 5	0.10	0.23
W4.8	He, 973 K	842 ± 5	0.16	0.30
W23.1	He, 973 K	584 ± 4	0.09	0.22
W4.8	He, 1223 K	792 ± 7	0.13	0.25
W23.1	He, 1223 K	555 ± 5	0.07	0.21

TABLE 2

Surface Area and Porosity of Support and Supported Catalysts from Series HW after Their Heat Treatments in He Flow at Different Temperatures for 4 h

Sample	Treatment	S_{N_2} , $m^2 g^{-1}$	V_2 , $cm^3 g^{-1}$	V_3 , $cm^3 g^{-1}$
S	—	929 ± 7	0.17	0.36
HW6.1	He, 748 K	907 ± 10	0.19	0.34
HW15.1	He, 748 K	696 ± 9	0.14	0.27
HW6.1	He, 1223 K	898 ± 11	0.15	0.29
HW15.1	He, 1223 K	552 ± 10	0.13	0.27

Chemical State and Dispersion of the Metallic Phase

The chemical state and dispersion of the metallic phase were studied by XRD and XPS after the supported catalysts were heat treated in He flow at different temperatures.

When ammonium tungstate is decomposed in an inert atmosphere tungsten trioxide is obtained, which has a ReO_3 structure and consists in a tridimensional network of octahedral WO_6 units sharing their corners (52). This tungsten trioxide is polymorphic and, therefore, can have different crystallographic forms depending on the temperature, the most stable at room temperature being the rhombic WO_3 . Results obtained when physical mixtures of WO_3 and carbon (in the form of graphite and lamp black) were heated in the temperature range 1208–1373 K have been reported recently by Venables and Brown (59, 60). The reduction was carried out isothermally in Ar flow. These authors propose a two-state reduction to W metal, via WO_2 . The rate of reduction depended on the temperature, the Ar flow, and the CO/CO_2 and WO_3 /carbon ratios. Between WO_3 and WO_2 different nonstoichiometric phases such as $W_{20}O_{58}$ and $W_{18}O_{49}$ appeared in which the metal was in two oxidation states (VI) and (IV). Their abundance in the reactant mixture depended on reaction time and temperature. Moreover, the above authors found that, although the original shape of the WO_3 particles was maintained, they became more porous when the molar volume of the phases diminished. Both the tungsten and tungsten trioxide particles had a certain mobility.

The reduction of WO_3 with CO at temperatures between 923 and 1173 K was also studied by the above authors (61).

The intermediate phases $W_{20}O_{58}$, $W_{18}O_{49}$, and WO_2 were observed in the reduction. The final product of the reaction was WC, compared with the tungsten formed when carbon was used. The supported catalysts used in this work were heated in He flow at 623, 748, 973, and 1223 K for 4 h. From a thermodynamic point of view (53), the reduction of WO_3 to WO_2 by the carbon support should be possible at 973 and 1223 K, whereas the reduction to W and formation of WC should be possible only at 1223 K. According to these data, the O/W atomic ratio diminishes when the temperature increases from 623 to 1223 K. Thus, in the case of the supported catalysts from series W, one would expect that at 623 and 748 K the metallic phase obtained would be essentially WO_3 , although the presence of some nonstoichiometric oxide with its O/W atomic ratio close to 3 could be possible. After the treatment at 973 K, a mixture of WO_3 nonstoichiometric oxides and WO_2 is expected. Finally, after the treatment at 1223 K, metallic W, WC, and probably some tungsten oxides would be expected.

Catalysts W9.1, W14.9, and W23.1 were analyzed by XRD after their heat treatments between 623 and 1223 K and the results found are compiled in Table 3. These results show that at 623 K two oxides WO_3 and $W_{25}O_{73}$ (O/W = 2.92) could be detected, at 748 K WO_3 and $W_{20}O_{58}$ appeared (O/W = 2.90), and at 973 K WO_3 , $W_{20}O_{58}$, and $W_{18}O_{49}$ appeared (O/W = 2.70). Therefore, the higher the treatment temperature the lower the O/W atomic ratio. When the catalysts were heat treated at 1223 K a mixture of metallic W, WC, and a nonstoichiometric carbide with composition $W_6C_{2.54}$ was obtained, which again confirms that the tungsten oxides were reduced by the carbon support to metallic tungsten at 1223 K, and that it reacted with the carbon support giving different carbides.

These results are quite interesting and show the important role that carbon materials can play as supports of metals that can yield carbides, since this could be a method to obtain metal carbides dispersed on a high surface area support. It is noteworthy that WO_2 was not detected after any of the heat treatments. This could indicate that the reduction of WO_3 , and the other nonstoichiometric oxides, was produced directly to W and not via WO_2 , in contrast to Venables and Brown's findings (59–61). Our results could be due to the higher dispersion that the tungsten oxides have on the activated carbon in comparison to that

TABLE 3

Tungsten Oxides Detected by XRD in Some Selected Catalysts of Series W Heat Treated in He Flow at Different Temperatures for 4 h

Sample	623 K	748 K	973 K	1223 K
W9.1	—	$WO_3(r) + W_{20}O_5$	$WO_3(r) + W_{20}O_{58} + W_{18}O_{49}$	$W + WC + W_6C_{2.54}$
W14.9	$WO_3(r) + W_{25}O_{73}$	$WO_3(r) + W_{20}O_5$	$WO_3(r) + W_{20}O_{58} + W_{18}O_{49}$	$W + WC + W_6C_{2.54}$
W23.1	$WO_3(r) + W_{25}O_{73}$	$WO_3(r) + W_{20}O_5$	$WO_3(r) + W_{20}O_{58} + W_{18}O_{49}$	$W + WC + W_6C_{2.54}$

obtained by the above authors, since they used a physical mixture of WO_3 with carbon.

XRD patterns of the heat-treated catalysts from series HW did not show any diffraction peaks corresponding to the metallic phase, except for samples treated at 973 K which showed small diffraction peaks corresponding to $\text{W}_{20}\text{O}_{58}$. These results indicate that, at this measuring scale, the metallic phase was well dispersed, forming either an amorphous phase or microcrystals smaller than 4.0 nm.

XPS spectra of the W_{4f} level for the catalysts W14.9 and HW15.1 studied after their heat treatments in He between 623 and 1223 K are shown in Figs. 5 and 6, as an example. These figures also include the curve-fitted spectra. The binding energies (BEs) of the $\text{W}_{4f_{7/2}}$ and the percentages of the different metallic species obtained from spectra similar

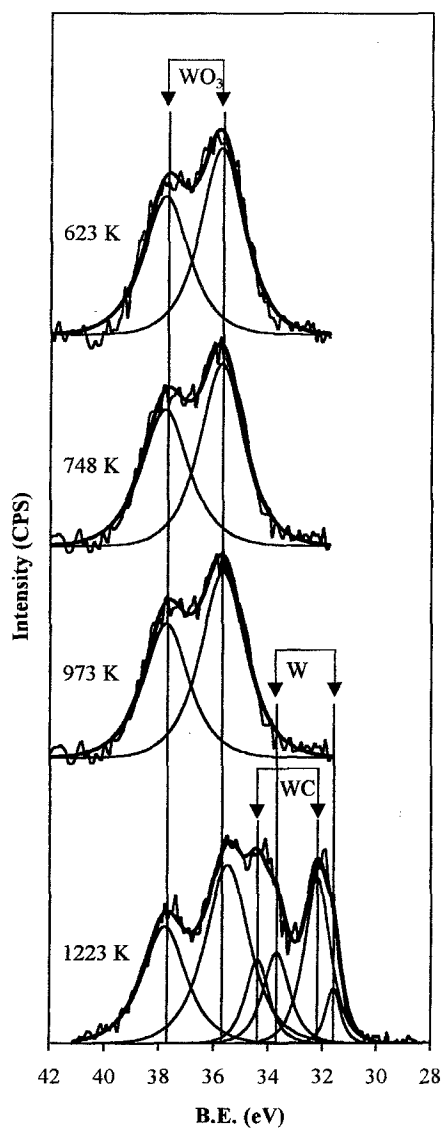


FIG. 5. Curve-fitted W_{4f} core-level spectra for catalyst W14.9 treated in He flow at different temperatures.

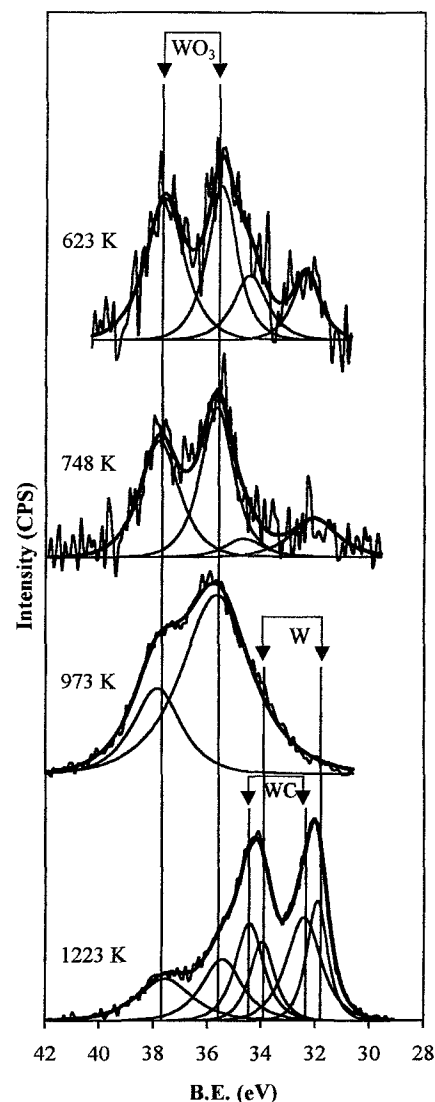


FIG. 6. Curve-fitted W_{4f} core-level spectra for catalyst HW15.1 treated in He flow at different temperatures.

to the one above are compiled in Table 4. These results indicate that for catalysts from the W series and HW6.1 heated between 623 and 973 K, tungsten was in oxidation state (VI) with BE at 35.5–35.8 eV. In the case of catalyst HW15.1, a small fraction of the tungsten hexacarbonyl appeared at a BE of 32.4–32.0 eV, which decreased when the treatment temperature increased. From the temperature-programmed decomposition experiments of these catalysts it was shown that decarbonylation of the tungsten hexacarbonyl was incomplete.

When the supported catalysts were heat treated at 1223 K a mixture of W (BE at 31.6–31.9 eV), WC (BE at 32.4–32.2 eV), and WO_3 was obtained. In both series of catalysts there was an increase in the percentages of W and WC and a decrease in the percentage of WO_3 when the tungsten

TABLE 4
BE Values (eV) of $W_{4f7/2}$ Core-Level Spectra for Catalysts Heat Treated in He Flow at Different Temperatures for 4 h^a

$T_{\text{treatment}}$, K	Catalyst				
	W4.8	W14.9	W23.1	HW6.1	HW15.1
623	35.6	35.8	35.6	35.5	32.4 (29) 35.5 (71)
748	35.5	35.7	35.6	35.6	32.0 (21) 35.7 (79)
973	35.7	35.7	35.7	35.5	35.7 (100)
1223	31.7 (7) 32.4 (16) 35.5 (77)	31.6 (7) 32.2 (33) 35.5 (60)	31.7 (25) 32.2 (40) 35.5 (35)	31.8 (13) 32.4 (25) 35.6 (62)	31.9 (29) 32.4 (41) 35.4 (30)

^a The values in parentheses correspond to percentage of each peak.

content of the catalysts increased. This WO_3 was not detected by XRD, probably because it was well dispersed on the support or in a thin layer covering the surface of the metallic particles. It has been demonstrated (15, 62, 63) that information about supported metallic particles can be obtained from the metal/support surface atomic ratio. Thus, Fig. 7 shows the relationships between the surface atomic ratio, $(W/C)_s$, and the total or bulk atomic ratio, $(W/S)_t$, for the catalysts from series W heat treated at different temperatures. The linear relationship found between the two magnitudes seems to indicate that the metallic phase is uniformly dispersed on the support along the concentration range studied.

The dependence of the $(W/C)_s$ ratio with the treatment temperature is shown in Figs. 8 and 9 for catalysts from series W and HW, respectively. For the catalysts from series W, the $(W/C)_s$ ratio practically did not change between 623 and 973 K, but increased when the temperature increased up to 1223 K. This was even more marked in catalysts with a high tungsten content, indicative of a surface segregation of the metallic phase. In the case of catalysts from series HW, the $(W/C)_s$ ratio did not change between 623 and 748 K, increasing for 973 K. This increase was very marked for sample HW15.1, indicative of a strong tungsten surface segregation was observed at a treatment temperature lower than that in series W. These results indicate that the tungsten species in series HW had a larger mobility than that in series W. Furthermore, the mobility increased in a larger proportion when the tungsten content increased.

The O_{1s} core-level spectra of the supported catalysts showed two components: the peak at 531.2 eV is due to W–O bonds in the WO_3 free (64) and also assigned to WO_3 monocrystals supported on SiO_2 (16, 65); the other peak above 533 eV is due to oxygen bonded to the support (66). On the other hand the peak at 531.2 eV could also

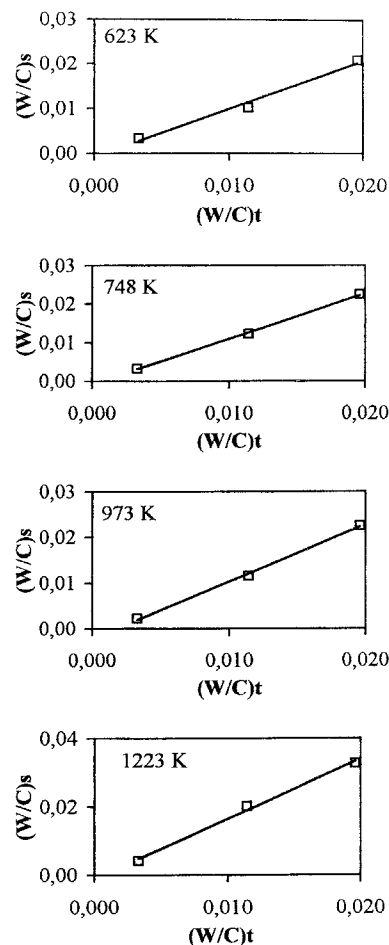


FIG. 7. Variation of surface atomic ratio, $(W/C)_s$, against total atomic ratio, $(W/C)_t$, for catalysts from series W treated at different temperatures.

be due to C=O bonds from the support, in ketones and carboxylic acids (66). However, the oxygen content of the support was very low, 2.2%, and the percentage of the peak at 531.2 eV was much lower than that at 533 eV, essentially

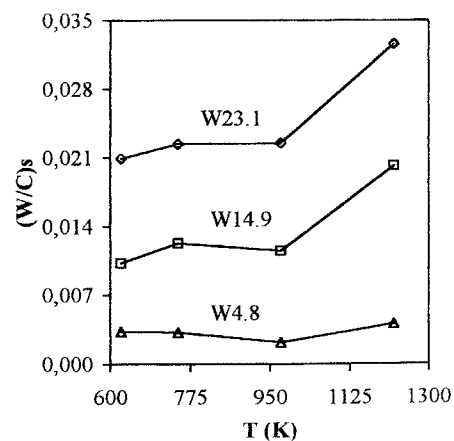


FIG. 8. Dependence of the treatment temperature on the W/C ratio for catalysts from series W.

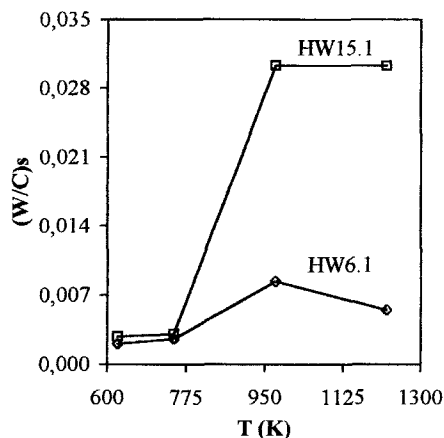


FIG. 9. Dependence of the treatment temperature on the W/C ratio for catalysts from series HW.

in the catalyst with the low tungsten content, which in turn would be similar to the support. Therefore, the peak at 531.2 eV would be essentially due to W–O bonds. The surface atomic ratios, (O/W)s, taking as reference the oxygen peak at 531.2 eV, in the case of the catalysts of both series as a function of treatment temperature, are compiled in Table 5. This ratio decreased when the treatment temperature increased and became lower than 3, essentially above 748 K. This implies that in the WO_3 particles tungsten atoms with an oxidation state lower than (VI) appeared, as shown by XRD. At 1223 K, the (O/W)s ratio was very low, since at this temperature there was a mixture of W, WC, and WO_3 .

Total Surface Acidity of the Supported Tungsten Catalysts

The total surface acidity of the supported tungsten catalysts was determined by TPD of ammonia previously adsorbed at 373 K and by studying the decomposition reaction of isopropanol. The acid surface properties of these catalysts are of major importance to determine their catalytic behavior (67). The acidic character of the tungsten oxide is well known (68, 69), and its acid strength is the highest among the metal oxides from groups 4, 5, and 6 of the Periodic Table and higher than those of Al_2O_3 and Re_2O_7 (68). Two types of acid sites are found on the surface of

TABLE 5

O/W Surface Atomic Ratio Taking as Reference the Oxygen Peak at 531.2 eV

$T_{\text{treatment}}$, K	Catalyst				
	W4.8	W14.9	W23.1	HW6.1	HW15.1
623	3.00	3.01	2.96	2.98	3.00
748	2.93	2.83	3.03	2.86	2.83
973	2.90	2.66	2.29	1.82	2.75
1223	0.93	1.09	0.93	0.82	1.00

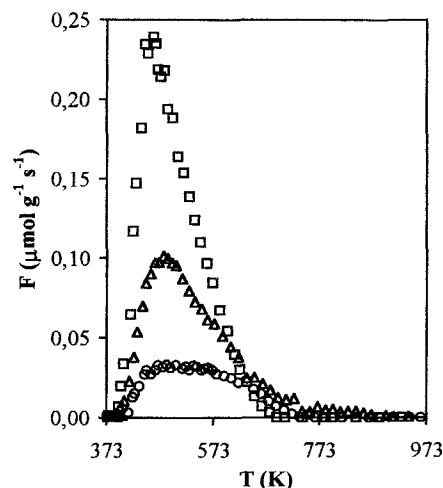


FIG. 10. TPD profiles of NH_3 from catalyst HW15.1 treated in He flow at different temperatures. \square , 623 K; \triangle , 973 K; \circ , 1223 K.

these metal oxides: Lewis and Brønsted. Lewis sites appear on metal atoms coordinatively unsaturated that can accept electrons. Brønsted type acid sites can supply protons to a base (69) and these are quite important in reactions such as catalytic cracking and in the skeletal isomerization of 1-butene to isobutene (67).

In general, it is accepted that NH_3 is an excellent molecular probe to measure the total surface acidity of catalysts, since due to its strong basicity and small molecular size, it allows the measurement of acid surface sites inside narrow pores (71–75). In this work, the adsorption process of NH_3 was carried out at 373 K in order to minimize adsorption on the support. Thus, after heat treatment of the support at 623 K in He flow for 4 h, it adsorbed a negligible amount of NH_3 at 373 K, and the amount adsorbed became zero when the treatment temperature increased. The NH_3 desorption profiles obtained with sample HW15.1 are shown in Fig. 10, as an example. Measurement of the total surface acidity was obtained from the area under these profiles, and these are compiled in Table 6, which shows that the amount of NH_3

TABLE 6

Amounts of NH_3 Desorbed ($\mu\text{mol g}^{-1}$) from the Supported Tungsten Catalysts Previously Heat Treated in He Flow at Different Temperatures

Catalyst	Treatment temperature			
	623 K	748 K	973 K	1223 K
W4.8	44	41	24	18
W9.1	69	58	47	32
W14.9	95	74	59	49
W23.1	139	112	68	53
HW6.1	53	48	24	21
HW15.1	173	147	92	41

desorbed and, therefore, the total surface acidity decreased when the treatment temperature increased.

The decrease in total surface acidity is due to a loss of both Lewis and Brønsted acid surface sites. We have shown before that the (O/W)s atomic ratio decreased when the treatment temperature increased. As a result, the oxidation state of some W atoms decreased to below (VI), producing a reduction in Lewis acidity. The increased treatment temperature produced a reduction in the Brønsted acidity due to the loss of -OH groups bonded to the surface W atoms and supplied by the support (probably from its humidity content). The high surface acidity of catalyst HW15.1 after the treatments between 623 and 748 K is noteworthy since this was much higher than that of catalyst W14.9. These results indicate again that the catalysts prepared from $W(CO)_6$ have a much higher dispersion than catalysts prepared from ammonium tungstate.

Many catalytic reactions have been used also to quantify the surface acidity of the catalysts (48). Ai *et al.* (76–81) related the catalytic activity of the metal oxides in different reactions with the acid–base character of their surface active sites, and propose the use of the decomposition reaction of isopropanol to indirectly determine this acid–base character. From a mechanistic point of view, Ai *et al.* (76–81) proposed that the dehydration of isopropanol is catalyzed by the acid sites and its dehydrogenation by both acid and basic sites. Therefore, and according to these authors, the rate of dehydration is a measurement of the total surface acidity, and the ratio between the rates of dehydrogenation and dehydration can be taken as a measurement of the total surface basicity.

Propene and acetone were the reaction products obtained with some selected catalysts and the activities to obtain both propene, r_p , and acetone, r_a , at 383 K are summarized in Table 7. The results show that r_p was much higher than r_a , and that r_p decreased when the treatment temperature increased. Therefore, the catalysts were essentially of

TABLE 7

Rates for Propene (r_p) and Acetone (r_a) Formation from Isopropanol Decomposition on Different Catalysts (Reaction Temperature 383 K)

Catalyst	$T_{\text{treatment, K}}$	$r_p, \mu\text{mol g}^{-1} \text{min}^{-1}$	$r_a, \mu\text{mol g}^{-1} \text{min}^{-1}$	r_a/r_p
W14.9	623	18.72	1.41	0.075
W14.9	748	9.78	0.71	0.073
W14.9	973	3.72	0.10	0.027
W23.1	623	29.52	1.59	0.054
W23.1	748	20.82	1.08	0.052
W23.1	973	6.48	0.19	0.029
HW15.1	623	48.30	2.27	0.047
HW15.1	748	32.88	1.15	0.035
HW15.1	973	17.88	0.61	0.034

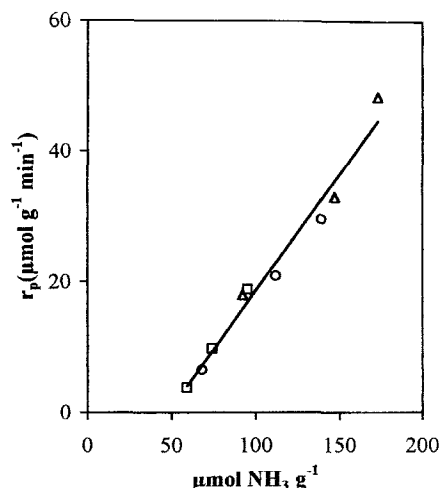


FIG. 11. Relationship between the rate of formation of propene and the total surface acidity measured by desorption of ammonia. □, W14.9; ○, W23.1; △, HW15.1.

acid character and this decreased, as shown before, when the treatment temperature increased. The r_a/r_p ratio is a measure of the basicity. This was very low and decreased further when the treatment temperature increased. Finally, Fig. 11 shows that there was a good linear relationship (correlation coefficient = 0.9741) between r_p and the amount of NH_3 desorbed, independent of both the catalyst series and the treatment temperature.

CONCLUSIONS

The surface area and porosity of the support decreased when the tungsten content of the supported catalysts increased. When the catalysts prepared from ammonium tungstate (series W) were heat treated between 623 and 973 K, rhombic WO_3 together with other nonstoichiometric oxides, in which the O/W ratio was lower than 3, were detected by XRD. Under the same conditions, the catalysts prepared from the tungsten hexacarbonyl (series HW) did not show any diffraction peak, implying that the metallic phase was well dispersed forming either an amorphous phase or microcrystals smaller than 4.0 nm. When the catalysts from series W were heat treated at 1223 K, a mixture of metallic tungsten and tungsten carbides was detected by XRD. Therefore, the support was able to reduce the tungsten oxides to metallic tungsten and react with it to produce different tungsten carbides. These results are quite interesting and show the important role that carbon materials can play as supports of metals that can yield carbides, by moderate heat treatments, since this could be a method to obtain metal carbides dispersed on a high surface area support. Catalysts prepared from series HW did not show any diffraction peak by XRD after heat treatments at 1223 K.

XPS showed a decrease in the O/W surface atomic ratio when the heat treatment temperature increased. In the case of the catalysts from series W there was a homogeneous distribution of the metallic phase in the range of metal content studied and at any treatment temperature. The W/C surface atomic ratio markedly increased with temperature between 973 and 1223 K in the catalysts from series W and between 748 and 973 K in the catalysts from series HW. This implies that the metallic phase was more mobile in the HW series.

Total surface acidity, as measured by NH₃ desorption, increased with tungsten content and decreased when treatment temperature increased due to the loss of surface acid sites of Lewis and Brønsted types. The high surface acidity of catalyst HW15.1 is noteworthy and is associated with the high dispersion of metal oxide. Decomposition of isopropanol yielded propene and acetone and the activity to produce propene was much higher than that to acetone. This implies that the catalysts were essentially of an acidic nature. The activity to produce propene decreased with the increase in treatment temperature and there was a linear relationship between this activity and the total acidity obtained by NH₃ desorption, irrespective the method of preparation of the catalysts and the treatment temperature applied.

ACKNOWLEDGMENTS

This work was supported by DGESIC Project no. PB97-0831.

REFERENCES

1. Thomas, C. L., "Catalytic Processes and Proven Catalysts." Academic Press, New York, 1970.
2. Moffet, A. J., Clark, A., and Johnson, M. M., *J. Catal.* **22**, 379 (1971).
3. Ai, M., *J. Catal.* **49**, 305 (1977).
4. Yamaguchi, T., Tanaka, Y., and Tanabe, K., *J. Catal.* **65**, 442 (1980).
5. Thomas, R., Van Oers, E. M., de Beer, V. H. J., Medema, J., and Mouljin, J. A., *J. Catal.* **76**, 241 (1982).
6. Wojciechowska, M., Gut, W., and Szymenderska, V., *Catal. Lett.* **7**, 431 (1990).
7. Gielgens, L. H., van Kampen, M. G. H., Broek, M. M., van Hardeveld, R., and Ponec, V., *J. Catal.* **154**, 201 (1995).
8. Rodríguez-Ramos, I., Guerrero-Ruiz, A., Homs, N., Ramírez de la Piscina, P., and Fierro, J. L. G., *J. Mol. Catal. A: Chem.* **95**, 147 (1995).
9. Martín, C., Rives, V., and Solana, G., *React. Kinet. Catal. Lett.* **58**, 243 (1996).
10. Ramírez, J., and Gutiérrez-Alejandre, A., *J. Catal.* **170**, 108 (1997).
11. Yori, J. C., Vera, C. R., and Parera, J. M., *Appl. Catal. A: Gen.* **163**, 165 (1997).
12. Yoshinaga, Y., Kudo, M., Hasegawa, S., and Okuhara, T., *Appl. Surf. Sci.* **121/122**, 339 (1997).
13. Ng, K. T., and Hercules, D. M., *J. Phys. Chem.* **80**, 2094 (1976).
14. Kerkhof, F. P., Mouljin, J. A., and Heeres, A., *J. Electron Spectrosc. Relat. Phenom.* **14**, 453 (1978).
15. Salvati, L., Makovsky, L. E., Stencel, J. M., Brown, F. R., and Hercules, D. M., *J. Phys. Chem.* **85**, 3700 (1981).
16. Murrell, L. L., Grenoble, D. C., Baker, R. T. K., Prestidge, E. B., Fung, S. C., Chianelli, R., and Cramer, S. P., *J. Catal.* **79**, 203 (1983).
17. Chan, S. S., Wachs, I. E., Murrell, L. L., Wang, L., and Hall, W. K., *J. Phys. Chem.* **88**, 5831 (1984).
18. Horsley, J. A., Wachs, I. E., Brown, J. M., Via, G. H., and Hardcastle, F. D., *J. Phys. Chem.* **91**, 4014 (1987).
19. Vermaire, D. C., and van Berge, P. C., *J. Catal.* **116**, 309 (1989).
20. Brady, R. L., Southmayd, D., Contescu, C., Zhang, R., and Schwarz, J. A., *J. Catal.* **129**, 195 (1991).
21. Vuurman, M. A., Wachs, I. E., and Hirt, A. M., *J. Phys. Chem.* **95**, 9928 (1991).
22. Hilbrig, F., Göbel, H. E., Knözinger, H., Schmelz, H., and Lengeler, B., *J. Phys. Chem.* **95**, 6973 (1991).
23. Ramis, G., Busca, G., Cristiani, C., Lietti, L., Forzatti, P., and Bregani, F., *Langmuir* **8**, 1744 (1992).
24. Vuurman, M. A., and Wachs, I. E., *J. Phys. Chem.* **96**, 5008 (1992).
25. Quincy, R. B., Houalla, M., and Hercules, D. M., *Fresenius J. Anal. Chem.* **346**, 676 (1993).
26. Mulcahy, F. M., Houalla, M., and Hercules, D. M., *J. Catal.* **139**, 72 (1993).
27. Colque, S., Payen, E., and Grange, P., *J. Mater. Chem.* **4**, 1343 (1994).
28. Pizzio, L. R., Cáceres, C. V., and Blanco, M. N., *Catal. Lett.* **33**, 175 (1995).
29. Marci, G., Palmisano, L., Sclafani, A., Venezia, A. M., Campostrini, R., Garturan, G., Martin, C., Rives, V., and Solana, G., *J. Chem. Soc., Faraday Trans.* **92**, 819 (1996).
30. Kim, D. S., Ostromecki, M., and Wachs, I. E., *J. Mol. Catal.* **106**, 93 (1996).
31. Wachs, I. E., *Catal. Today* **27**, 437 (1996).
32. Martín, C., Malet, P., Rives, V., and Solana, G., *J. Catal.* **169**, 516 (1997).
33. Radovic, I. R., and Rodríguez-Reinoso, F., in "Chemistry and Physics of Carbon" (P. A. Thrower, Ed.), Vol. 25, p. 243. Dekker, New York, (1997).
34. Moreno-Castilla, C., Maldonado-Hódar, F., Rivera-Utrilla, J., and Rodríguez-Castellón, E., *Appl. Catal. A: Gen.* **183**, 345 (1999).
35. Duchet, J. C., van Oers, E. M., de Beer, V. H. J., and Prins, R., *J. Catal.* **80**, 386 (1983).
36. López-Ramón, M. V., Moreno-Castilla, C., Rivera-Utrilla, J., and Hidalgo-Alvarez, R., *Carbon* **31**, 815 (1993).
37. Moreno-Castilla, C., Salas-Peregrín, M. A., and López-Garzón, F. J., *J. Mol. Catal. A: Chem.* **95**, 223 (1995).
38. Moreno-Castilla, C., Salas-Peregrín, M. A., and López-Garzón, F. J., *Fuel* **74**, 830 (1995).
39. López-Ramón, M. V., Stoeckli, F., Moreno-Castilla, C., Carrasco-Marín, F., *Carbon* **37**, 1215 (1999).
40. Ferro-García, M. A., Utrera-Hidalgo, E., Rivera-Utrilla, J., Moreno-Castilla, C., and Joly, J. P., *Carbon* **31**, 857 (1993).
41. Soled, S. L., McVicker, G. B., Murrell, L. L., Sherman, L. G., Dispenziere, N. C., Hsu, S. L., and Waldman, D., *J. Catal.* **111**, 286 (1988).
42. Papadopoulou, Ch., Matralis, H., Lycourghiotis, A., Grange, P., and Delmon, B., *J. Chem. Soc., Faraday Trans.* **89**, 3157 (1993).
43. Simon, M. W., Suib, S. L., and O'Young, C. L., *J. Catal.* **147**, 484 (1994).
44. Xu, W. Q., Yin, Y. G., Suib, S. L., and O'Young, C. L., *J. Catal.* **150**, 14 (1994).
45. Karakonstantis, L., Mastralis, H., Kordulis, Ch., and Lycourghiotis, A., *J. Catal.* **162**, 306 (1996).
46. Baeck, S. Y., and Lee, W. Y., *Appl. Catal. A* **168**, 171 (1998).
47. Arena, F., Dario, R., and Parmaliana, A., *Appl. Catal.* **170**, 127 (1998).
48. Gervasini, A., and Auroux, A., *J. Catal.* **131**, 190 (1991).
49. Afanasiev, P., Geantet, C., Breysse, M., Coudurier, G., and Vedrine, J. C., *J. Chem. Soc., Faraday Trans.* **90**, 193 (1994).
50. Gervasini, A., Bellussi, G., Fenyvesi, J., and Auroux, A., *J. Phys. Chem.* **99**, 5117 (1995).
51. Aramendía, M. A., Boráu, V., Jiménez, C., Marinas, J. M., Porras, A., and Urbano, F. J., *J. Chem. Soc., Faraday Trans.* **93**, 1431 (1997).
52. Greenwood, N. N., and Earnshaw, A., "Chemistry of the Elements," 2nd ed., Chap. 23, p. 1167. Butterworth-Heinemann, Oxford, 1997.

53. Kubachewski, O., Evans, E. L., and Alcock, C. R., "Metallurgical Thermochemistry," 4th ed. Pergamon, New York, 1967.
54. González, P. N., Villa-García, M. A., and Brenner, A., *J. Catal.* **118**, 360 (1989).
55. Brenner, A., and Burwell, R. L., *J. Catal.* **52**, 353 (1978).
56. Hucul, D. A., and Brenner, A., *J. Catal.* **61**, 216 (1980).
57. Hucul, D. A., and Brenner, A., *J. Chem. Soc., Chem. Commun.* 830 (1982).
58. Gregg, S. J., and Sing, K. S. W., "Adsorption Surface Area and Porosity," 2nd ed. Academic Press, London, 1982.
59. Venables, D. S., and Brown, M. E., *Thermochim. Acta* **282/283**, 251 (1996).
60. Venables, D. S., and Brown, M. E., *Thermochim. Acta* **282/283**, 265 (1996).
61. Venables, D. S., and Brown, M. E., *Thermochim. Acta* **291**, 131 (1997).
62. Kerkhof, F. P. J. M., and Moulijn, J. A., *J. Phys. Chem.* **83**, 1612 (1979).
63. Fung, S. C., *J. Catal.* **58**, 454 (1979).
64. Wills, G. B., Fathikalajahi, J., Gangwal, S. K., and Tang, S., *Recl. Trav. Chim. Pays-Bas* **96**, M110 (1977).
65. Verpoort, F., Fiermans, L., Bossuyt, A. R., and Verdonck, L., *J. Mol. Catal.* **90**, 43 (1994).
66. Desimoni, E., Casella, G. I., and Salvi, A. M., *Carbon* **30**, 521 (1992).
67. Carniti, P., Gervasini, A., and Auroux, A., *J. Catal.* **150**, 274 (1994).
68. Bernholc, J., Horsley, J. A., Murrell, L. L., Sherman, L. G., and Soled, S., *J. Phys. Chem.* **91**, 1526 (1987).
69. Houzvicka, J., and Ponec, V., *Catal. Rev.-Sci. Eng.* **39**, 319 (1997).
70. Boorman, P. M., Kriz, J. F., Brown, J. R., and Ternan, M., "Proceedings, 8th International Congress on Catalysis," Berlin, 1984, Vol. II. Verlag-Chemie, Berlin, 1984.
71. Hidalgo, C. V., Itoh, H., Hattori, T., Niwa, M., and Murakami, Y., *J. Catal.* **85**, 362 (1984).
72. Kapustin, G. I., Brueva, T. R., Klyachko, A. L., Beran, S., and Wichterlova, B., *Appl. Catal.* **42**, 239 (1988).
73. Karge, H. G., and Dondur, V., *J. Phys. Chem.* **94**, 765 (1990).
74. Karge, H. G., Dondur, V., and Weitkamp, J., *J. Phys. Chem.* **95**, 283 (1991).
75. Abelló, M. C., Velasco, A. P., Gómez, M. F., and Rivarola, J. B., *Langmuir* **13**, 2596 (1997).
76. Ai, M., and Suzuki, S., *J. Catal.* **30**, 362 (1973).
77. Ai, M., *J. Catal.* **40**, 318 (1975).
78. Ai, M., *J. Catal.* **40**, 327 (1975).
79. Ai, M., and Ikawa, T., *J. Catal.* **40**, 203 (1975).
80. Ai, M., *Bull. Chem. Soc., Jpn.* **49**, 1328 (1976).
81. Ai, M., *Bull. Chem. Soc., Jpn.* **50**, 2579 (1977).